

Surface-Induced Hydrogelation Inhibits Platelet Aggregation

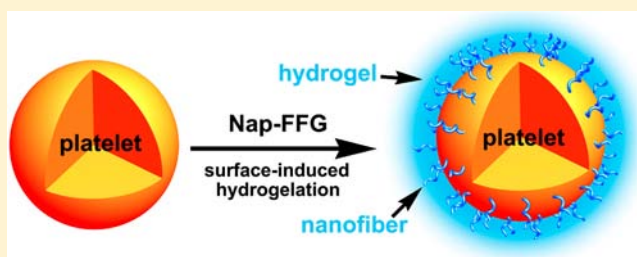
Wenting Zheng,^{†,‡} Jie Gao,^{†,‡} Lijie Song,[†] Chongyi Chen,[§] Di Guan,[†] Zhihong Wang,[†] Zhibo Li,^{*,§} Deling Kong,^{*,†} and Zhimou Yang^{*,†}

[†]State Key Laboratory of Medicinal Chemical Biology and College of Life Sciences, Nankai University, Tianjin 300071, P. R. China

[§]Institute of Chemistry, Chinese Academy of Sciences, Beijing 100190, P. R. China

Supporting Information

ABSTRACT: We demonstrate that a tripeptide hydrogelator, Nap-FFG, can selectively self-assemble at the surface of platelets, thus inhibiting ADP-, collagen-, thrombin- and arachidonic acid (AA)-induced human platelet aggregations with the IC₅₀ values of 0.035 (41), 0.14 (162), 0.062 (68), and 0.13 mg/mL (148 μM), respectively. Other tripeptide hydrogelators with chemical structures of Nap-FFX (X = A, K, S, or E) could not or possessed less potencies to inhibit platelet aggregations. We observed higher amounts of Nap-FFG at the platelet surface by the techniques of LC-MS and confocal microscopy. We also observed self-assembled nanofibers around the platelet incubated with the Nap-FFG by cryo-TEM. The ζ potential of Nap-FFG treated platelets was a little bit more negative than that of untreated ones. The amount of Nap-FFG at the surface of NIH 3T3 cells was much less than that of platelets. These observations suggested that Nap-FFG could selectively self-assemble through unknown ligand–receptor interactions and form thin layers of hydrogels at the surface of platelets, thus preventing the aggregation of them. This study not only broadened the application and opened up a new door for biomedical applications of molecular hydrogels but also might provide a novel strategy to counteract infection diseases through selective surface-induced hydrogelations at pathogens, such as bacteria and virus.



INTRODUCTION

Over the last two decades, molecular hydrogels^{1–4} have shown big potential in applications of sensing,^{5–8} drug delivery,^{9–15} tissue engineering,^{16–20} etc. Recently, their applications in biological fields attracted extensive research interests. For example, Stupp and Schneider groups demonstrated that self-assembled peptides could selectively form pores at the surface of cancer cells, thus resulting in cancer cells death.^{21,22} Collier and co-workers have shown that self-assembled peptides could be used as immune adjuvants.^{23,24} Xu group has conducted an assay to discover the interaction between proteins in the cell lysate and nanofibers of molecular gelators.²⁵ These successful results stimulated research interests and efforts to investigate the novel applications of molecular hydrogels in biological fields. In this paper, we demonstrated that a tripeptide hydrogelator, Nap-FFG, could selectively self-assemble at the surface of platelets. This surface-induced self-assembly could then inhibit human platelet aggregations induced by adenosine diphosphate (ADP), collagen, thrombin, and arachidonic acid (AA).

RESULTS AND DISCUSSION

Platelet Aggregation Inhibition Studies. We recently observed that a hydrogelator, Nap-FFGRGD, could self-assemble at the surface of fibril structures of polycaprolactone (PCL) prepared by electron spinning.^{26,27} We observed that surface-functionalized PCL could inhibit platelet adhesion. We

first thought that this inhibition was due to the presence of RGD tripeptide because RGD-containing peptides and proteins could inhibit platelet aggregation as they block the binding of fibrinogen to $\alpha_{IIb}\beta_3$ integrin.^{28,29} We then synthesized a control peptide of Nap-FFG to check whether it could inhibit platelet aggregation or not. Surprisingly, in an ADP-induced platelet aggregation assay, Nap-FFG exhibited a similar IC₅₀ value to Nap-FFGRGD (0.035 and 0.039 mg/mL for Nap-FFG and Nap-FFGRGD, respectively, Figure 1, top). The peptide of FGRGD showed no inhibition effects on platelet aggregation. These observations indicated that the inhibition effect of Nap-FFGRGD was not due to the presence of RGD.

We then designed and synthesized other short peptides with similar chemical structures to Nap-FFG and test their inhibition ability to against platelet aggregation. The peptide of Nap-FF showed no inhibition effects on platelet aggregation, indicating the importance of terminal G residue. The self-assembled peptides of FF and FFG also exhibited no inhibition effects, suggesting that hydrogelation ability of Nap-FFG might be important to the activity (FF and FFG could only form precipitations of nanotubes or nanospheres in aqueous solutions).^{30,31} We also altered the terminal G residue on Nap-FFG to other amino acids of alanine (A), serine (S), glutamic acid (E), and lysine (K). Nap-FFA possessed a slightly

Received: September 1, 2012

Published: December 14, 2012

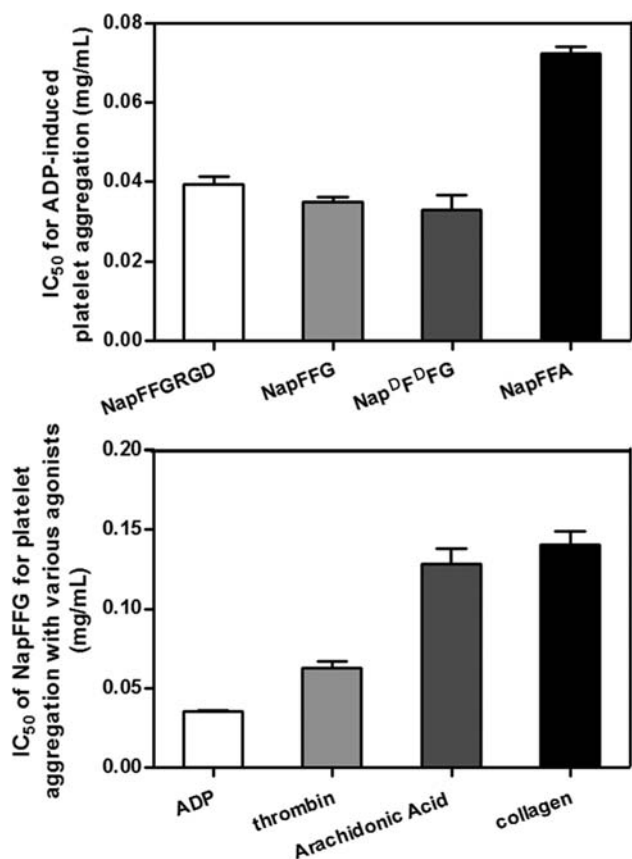


Figure 1. (top) Effects of different molecules on inhibition of platelet aggregation. (down) Effects of NapFFG on inhibition of platelet aggregation with various agonists (data were expressed as the mean \pm standard error of the mean (SEM), $N = 3$).

bigger IC₅₀ value (0.073 mg/mL) than Nap-FFG. Peptides of Nap-FFS, Nap-FFE, and Nap-FFK showed no inhibition effects on the platelet aggregation. These results indicated that the small side chains on G and A were crucial for the activity. The enantiomer of Nap-FFG, Nap-^DF^DFG, showed a very similar IC₅₀ value (0.033 mg/mL) to Nap-FFG. Based on the above information, we hypothesized that the hydrogelation ability and terminal amino acid with small side chains of the peptides were crucial for their activity against platelet aggregation.

To investigate the biological functions of Nap-FFG, we focused on its effect on platelet aggregation using various platelet aggregation agonists. Surprisingly, Nap-FFG inhibited collagen-, thrombin-, and AA- as well as ADP-induced human platelet aggregations. The IC₅₀ of Nap-FFG for collagen-, thrombin- and AA-induced platelet aggregation was 0.14 mg/mL (162 μ M), 0.062 mg/mL (68 μ M), and 0.128 mg/mL (148 μ M), respectively (Figure 1, down). There are some discoveries of platelet receptors, such as the ADP receptor and the GP IIb/IIIa complex.³² Many of the platelet receptors have been and are being developed as targets for preventing clot formation.³³ However, our results indicated that Nap-FFG was not targeting a particular platelet receptor. Since there were no detectable binding constants between Nap-FFG and the four platelet aggregation agonists determined by isothermal titration calorimetry (ITC, Figure S-13), the different IC₅₀ values of Nap-FFG were probably due to the different binding constants of Nap-FFG to the receptors of the agonists.

Liquid Chromatography Mass Spectrometry (LC-MS).

In order to test the affinity of different peptides to the platelet, we first incubated the platelet in solutions containing different kinds of peptides for 5 min and then separated the platelet from peptide solutions by centrifuge. The pellet was sonicated and suspended in DMSO. The resulting solution was then used for LC-MS analysis. As shown in Figure 2, more amounts of

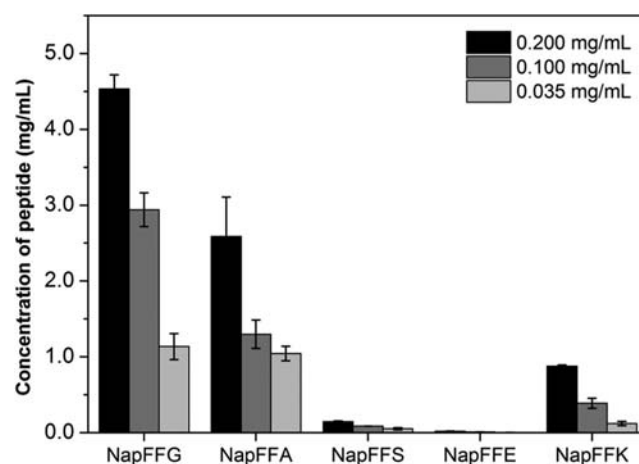


Figure 2. Amount of peptides in the centrifuged pellets was confirmed by LC-MS (data were expressed as the mean \pm SEM ($N = 3$)).

peptides were observed from the pellet when higher concentrations of peptides were used. Upon incubation with solutions containing the same concentration of different peptides, it was obviously observed that the amount of peptide in the pellet followed the trend of Nap-FFG > Nap-FFA \gg Nap-FFK/S/E, which was consistent to the trend of their ability to inhibit platelet aggregation. Since the solubility of all peptides in DMSO was higher than 100 mg/mL, the different amounts of peptides in the separated platelets were due to their different binding affinities to the platelets.

Self-Assembly Ability. In order to test whether the selective platelet aggregation inhibition ability and more amount of Nap-FFG in pellets were due to its different self-assembly property to other short peptides, we studied the hydrogelation ability of peptides and obtained their critical micelle concentrations (CMC). The results in Figure 3 showed that peptides of Nap-FFX except Nap-FFE could form hydrogels at

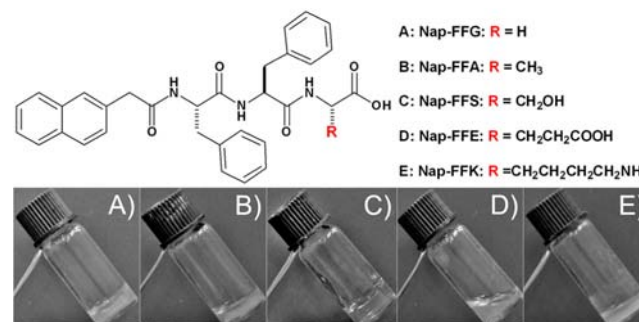


Figure 3. Chemical structures of short peptides used in this study and optical images of gels of peptides at the concentration of 1 wt %: (A) Nap-FFG, (B) Nap-FFA, (C) Nap-FFS, and (E) Nap-FFK. Nap-FFE cannot form gels at concentrations lower than 4 wt %, as shown in (D).

concentrations lower than 1 wt %. Nap-FFE could not form gels at concentrations lower than 4.0 wt % in PBS buffer (pH 7.4). The minimum gelation concentration (MGC) of Nap-FFG, Nap-FFA, Nap-FFS, and Nap-FFK was 0.3, 0.5, 0.08, and 0.2 wt %, respectively. The four gelators possessed similar CMC values and were 0.025, 0.025, 0.050, and 0.084 mg/mL for Nap-FFK, Nap-FFA, Nap-FFS, and Nap-FFG, respectively (Figure S-14). The similar self-assembly property of Nap-FFG to the other peptides, in combine with the result of more amounts of Nap-FFG in centrifuged pellets, suggested that the selective platelet aggregation inhibition of Nap-FFG was due to its selective binding to platelets.

Laser Scanning Confocal Microscopy. Thioflavin T has been applied to stain self-assembled nanofibers of short peptides.³⁴ In order to test whether Nap-FFG could form nanofibers at the surface of platelets or not, we incubated the platelet in the solution containing Nap-FFG and Thioflavin T and then obtained fluorescence images by confocal microscopy. As shown in Figure 4A,D (fluorescence, fluorescence + bright

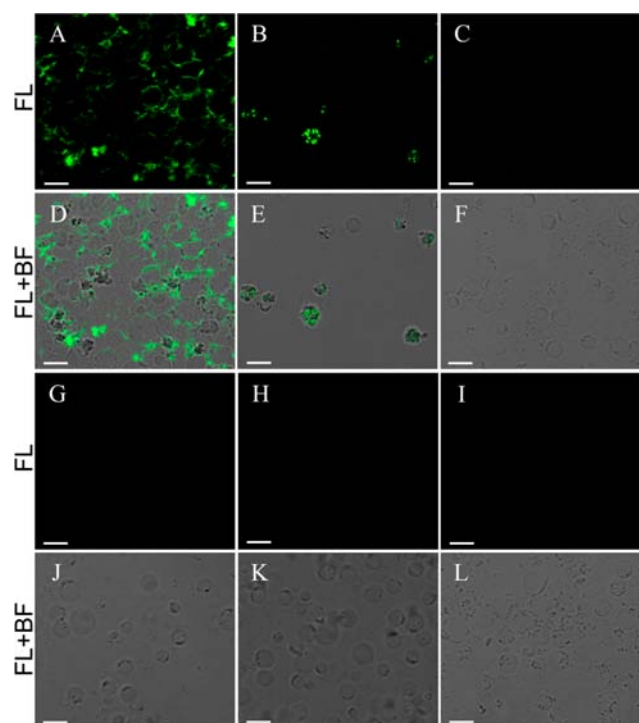


Figure 4. Fluorescence confocal microscopy images of platelets with peptides of Nap-FFG (A,D), Nap-FFA (B,E), Nap-FFS (C,F), Nap-FFE (G,J), and Nap-FFK (H,K) stained with Thioflavin T. Fluorescence microscopy images of platelets with Thioflavin T (L) and Nap-FFG solution with Thioflavin T (I). Scale bars, 5 μm . FL, fluorescence. BF, bright field. Peptide concentration was 0.2 mg/mL.

field, respectively), the platelets exhibited high intensities of fluorescence around them in the presence of Nap-FFG. Platelets incubated with the peptide of Nap-FFA also exhibited weak fluorescence but existing as unevenly distributed dots (Figure 4B,E). In the presence of Thioflavin T, the platelets without peptides (Figure 4L) and with other peptides and Nap-FFG solution without platelets (Figure 4I) showed no fluorescence. These observations clearly indicated that Nap-FFG could selectively self-assemble at the surface of platelets.

Cryo-Transmission Electron Microscopy (Cryo-TEM). Cryo-TEM images could show original structures of self-

assembled nanofibers in aqueous solutions. Therefore, we obtained cryo-TEM images of platelets incubated with/without peptides (Figure 5). The images in Figure 5A,B clearly

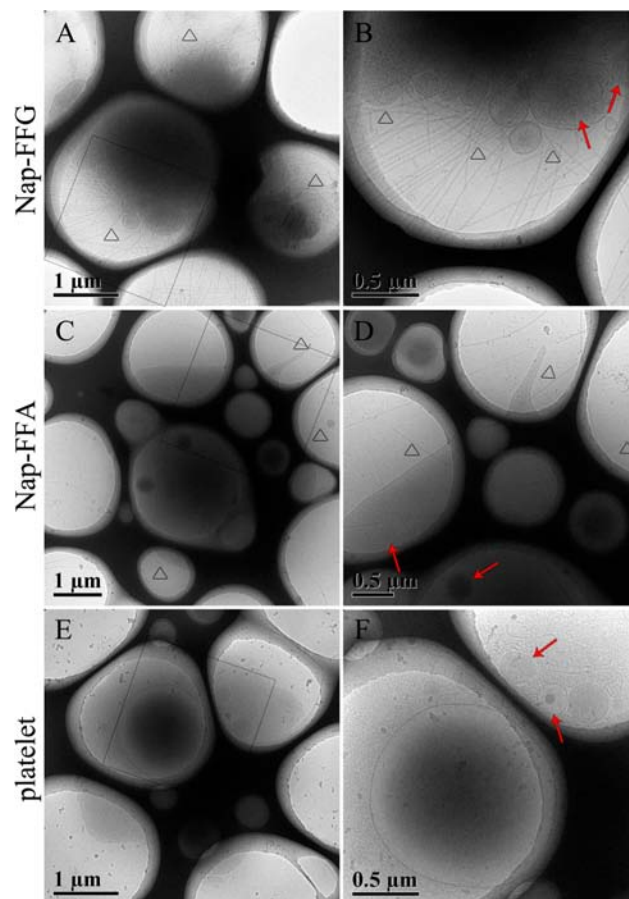


Figure 5. Cryo-TEM images of platelets with 0.2 mg/mL of NapFFG (A,B), NapFFA (C,D) and without peptides (E,F). Image of B, D, and F corresponds to the squares in image A, C, and E, respectively. Red arrows point out organelles of platelets, and triangles point out nanofibers.

indicated the presence of self-assembled nanofibers around the platelet treated with Nap-FFG, as pointing out by the open triangles. While in platelets treated with Nap-FFA, a smaller amount of nanofibers could be observed around the platelets (Figure 5C,D), and no fibers could be observed around platelets without peptides (Figure 5E,F) and with other peptides. These observations further demonstrated that Nap-FFG could selectively self-assemble at the surface of platelets.

Selectivity of Binding to Platelets. In order to test the selectivity of binding of Nap-FFG to platelets, we also incubated NIH 3T3 cells with different concentrations of the peptide (0.2, 0.1, and 0.035 mg/mL). In the centrifuged pellets of 3T3 cells, the concentrations of Nap-FFG were lower than 0.4 mg/mL for samples treated with three concentrations of Nap-FFG (0.2, 0.1, and 0.035 mg/mL, Figure S-15). Upon the treatment with 0.035 mg/mL of Nap-FFGRGD, the concentration of Nap-FFGRGD in centrifuged 3T3 cells was 1.76 mg/mL, indicating that RGD peptide could promote the binding of peptide to the cells through binding to the $\alpha_{\text{IIb}}\beta_3$ integrin. For centrifuged platelets (Figure 2), these values were 4.5, 2.9, and 1.2 mg/mL for samples treated with 0.2, 0.1, and 0.035 mg/mL of Nap-FFG, respectively. These differences suggested that

platelets would selectively absorb Nap-FFG and induce its self-assembly. While 3T3 cells could probably nonspecifically absorb the peptide because there were no differences in concentration of Nap-FFG in centrifuged 3T3 cells upon treated with different concentrations of the peptide.

Inhibition Mechanism. Based on the above information, we proposed a possible inhibition mechanism. As shown in Figure 6, Nap-FFG could selectively bind to the surface of

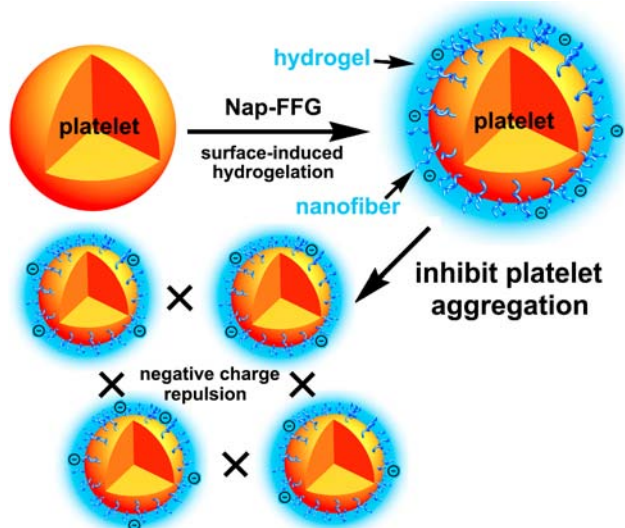


Figure 6. A possible mechanism of surface-induced hydrogelation of Nap-FFG to inhibit platelet aggregation by negative charge repulsion.

platelet through unknown ligand–receptor interactions, initiating the self-assembly of Nap-FFG and hydrogelation around the surface of platelet. This surface-induced hydrogelation³⁵ process might finished very rapidly (within one minute), as demonstrating by the similar inhibition percentages at different incubation times (1, 5, and 30 min, Figure S-16). The binding of Nap-FFG to platelet was crucial to the surface-induced hydrogelation because Nap-FFS/K with similar CMC values to Nap-FFG could not bind to platelet and form hydrogels around the platelet. Since the ζ potentials of all solutions of peptides were negative (Figure S-17), the thin layer of hydrogel of Nap-FFG around the platelet could make the ζ potential of treated platelets more negative (Figure S-18), thus preventing the aggregation of platelet by negative charge repulsion.

CONCLUSION

In summary, we have demonstrated that the tripeptide gelator of Nap-FFG could selectively self-assemble and form a thin layer of hydrogel at the surface of platelets, thus preventing the human platelet aggregation induced by different kinds of agonists. The binding of Nap-FFG to platelets was very tight, and Nap-FFG could not be washed off from the surface of the platelets even by washing 10 times with PBS or by washing 3 times with PBS containing 10 wt % of bovine serum albumin (BSA), 1 wt % of FFG or 1 wt % of FG. This study broadens the application of molecular hydrogelators in biological field. By improving the selectivity of the binding of gelators, it also provides a novel strategy to inhibit thrombus formation and may counteract infection diseases through selective surface-induced hydrogelation around the different kinds of pathogens, such as bacteria and virus.

EXPERIMENTAL SECTION

Chemicals and Materials. Fmoc amino acids were obtained from GL Biochem (Shanghai). All the other starting materials were obtained from Alfa. Commercially available reagents and solvents were used without further purification, unless noted otherwise. The synthesized compounds were characterized by ¹H NMR (Bruker ARX-300) using DMSO-*d*₆ as the solvent. HPLC was conducted at LUMTECH HPLC (Germany) system using a C₁₈ RP column with MeOH (0.05% of TFA) and water (0.05% of TFA) as the eluents. LC-MS was conducted at the LCMS-20AD (Shimadzu) system, HR-MS was performed at the Agilent 6520 Q-TOF LC/MS using ESI-L low-concentration tuning mix (lot no. LB60116 from the Agilent Tech.).

Peptide Synthesis. The peptide derivative was prepared by solid-phase peptide synthesis (SPPS) using 2-chlorotriyl chloride resin and the corresponding N-Fmoc-protected amino acids with side chains properly protected by a *tert*-butyl group or Pbf group. During deprotection of Fmoc group, 20% piperidine in anhydrous *N,N'*-dimethylformamide (DMF) was used. Then the next Fmoc-protected amino acid was coupled to the free amino group using *O*-(benzotriazol-1-yl)-*N,N,N',N'*-tetramethyluroniumhexafluorophosphate (HBTU) as the coupling reagent. The growth of the peptide chain was according to the established Fmoc SPPS protocol. After the last coupling step, excessive reagents were removed by a single DMF wash for 5 min (5 mL per gram of resin), followed by five steps of washing using DCM for 2 min (5 mL per gram of resin). The peptide derivative was cleaved using 95% of trifluoroacetic acid with 2.5% of trimethylsilane (TMS) and 2.5% of H₂O for 30 min. Twenty mL per gram of resin of ice-cold diethylether was then added to cleavage reagent. The resulting precipitate was centrifuged for 10 min at 4 °C at 10 000 rpm. Afterward the supernatant was decanted, and the resulting solid was dissolved in DMSO for HPLC separation using MeOH and H₂O containing 0.1% of TFA as eluents.

Characterization of the Peptides. The assignment of ¹H NMR peaks was in the ESI.

Nap-FFG. ¹H NMR (300 MHz, DMSO-*d*₆): δ 8.50–8.05 (m, 3H, N–H), 7.99–7.65 (m, 3H, Ar–H), 7.57 (s, 1H, Ar–H), 7.51–7.34 (m, 2H, Ar–H), 7.31–7.03 (m, 11H, Ar–H), 4.53 (m, 2H), 3.78 (d, *J* = 5.8 Hz, 2H), 3.52 (dd, *J* = 28.0, 14.0 Hz, 2H), 3.10–2.92 (m, 2H, –CH₂Ph), 2.76 (ddd, *J* = 28.9, 13.7, 9.8 Hz, 2H, –CH₂Ph). HR-MS: calcd *M*⁺ = 537.2336, obsvd (*M* + *H*)⁺ = 538.2332.

Nap-FFA. ¹H NMR (300 MHz, DMSO-*d*₆): δ 8.52–8.06 (m, 3H, N–H), 7.93–7.68 (m, 3H, Ar–H), 7.57 (s, 1H, Ar–H), 7.50–7.35 (m, 2H, Ar–H), 7.32–6.95 (m, 11H, Ar–H), 4.55 (m, 2H), 4.26–4.14 (m), 3.52 (dd, *J* = 28.4, 14.0 Hz, 2H), 3.01 (dd, *J* = 26.1, 10.5 Hz, 2H, –CH₂Ph), 2.85–2.65 (m, 2H, –CH₂Ph), 1.29 (d, *J* = 7.2 Hz, 3H, CH₃–). HR-MS: calcd *M*⁺ = 551.2493, obsvd (*M* + *H*)⁺ = 552.2491.

Nap-FFS. ¹H NMR (300 MHz, DMSO-*d*₆): δ 8.38–8.08 (m, 3H, N–H), 7.91–7.66 (m, 3H, Ar–H), 7.56 (s, 1H, Ar–H), 7.51–7.37 (m, 2H, Ar–H), 7.27–7.13 (m, 11H, Ar–H), 4.64 (dd, *J* = 10.5, 7.0 Hz, 1H), 4.50 (m, 1H), 4.30 (dd, *J* = 8.0, 4.4 Hz, 1H), 3.69 (ddd, *J* = 14.8, 10.8, 4.5 Hz, 2H, CH₂OH), 3.60–3.46 (m, 2H), 3.02 (ddd, *J* = 17.1, 14.0, 3.8 Hz, 2H, –CH₂Ph), 2.75 (ddd, *J* = 32.4, 13.7, 10.1 Hz, 2H, –CH₂Ph). HR-MS: calcd *M*⁺ = 567.2442, obsvd (*M* + *H*)⁺ = 568.2439.

Nap-FFK. ¹H NMR (300 MHz, DMSO-*d*₆): δ 8.30 (d, *J* = 6.0 Hz, 2H, N–H), 8.15 (d, *J* = 9.0 Hz, 1H, N–H), 7.85–7.71 (m, 3H, Ar–H), 7.56 (s, 1H, Ar–H), 7.51–7.40 (m, 2H, Ar–H), 7.34–7.06 (m, 11H, Ar–H), 4.54 (m, 2H), 4.20 (d, *J* = 4.6 Hz), 3.52 (dd, *J* = 30.4, 14.0 Hz, 2H), 3.09–2.92 (m, 2H, –CH₂Ph), 2.76 (ddd, *J* = 31.0, 18.9, 11.4 Hz, 4H), 1.62 (ddd, *J* = 25.6, 22.1, 7.3 Hz, 4H, –CH₂CH₂–), 1.36 (m, 2H, –CH₂–). HR-MS: calcd *M*⁺ = 608.3071, obsvd (*M* + *H*)⁺ = 609.3064.

Nap-FFE. ¹H NMR (300 MHz, DMSO-*d*₆): δ 8.25 (m, 3H, N–H), 7.88–7.64 (m, 3H, Ar–H), 7.56 (s, 1H, Ar–H), 7.45 (m, 2H, Ar–H), 7.33–6.97 (m, 11H, Ar–H), 4.53 (m, 2H), 4.26 (m, 1H), 3.51 (dd, *J* = 29.9, 11.2 Hz, 2H), 3.09–2.92 (m, 2H, –CH₂Ph), 2.85–2.65 (m, 2H, –CH₂Ph), 2.29 (d, *J* = 7.4 Hz, 2H, –CH₂COOH), 2.00 (m, 1H), 1.82 (m, 1H). HR-MS: calcd *M*⁺ = 609.2548, obsvd (*M* + *H*)⁺ = 610.2542.

Hydrogel Formation. 1.0 mg of each peptide and equal molar of sodium carbonate to the peptide were first suspended in PBS buffer (pH = 7.4); the sodium carbonate was used to neutralize the terminal carboxylic acid of peptides. The suspensions were then heated to 80 °C to form clear solutions. The gels would form after cooling back to room temperature within 3 min.

CMC. CMC values of peptides in PBS buffer solutions were determined by dynamic light scattering (DLS). Solutions containing different concentration of peptides were tested, and the light scattering intensity was recorded for each concentration analyzed. DLS was performed on a laser light scattering spectrometer (BI-200SM) equipped with a digital correlator (BI-9000AT) at 532 nm under room temperature (22–25 °C).

Preparation of Platelet-Rich Plasma (PRP) for Platelet Aggregation Inhibition Study. Briefly, fresh blood obtained from healthy donors was centrifuged at 175g for 10 min at 22 °C, and PRP was obtained. Fresh platelet preparations could be used for aggregation studies for as long as 6–8 h. The concentration of fresh PRP was 10⁷/mL.

Platelet Aggregation Inhibition Studies. Aggregation was measured at 37 °C by a turbidimetric method in a Chrono-Log platelet aggregometer (Chrono-Log Corporation, Havertown, PA). A 450 μL aliquot of PRP was stirred at 1100 rpm and activated by addition of different agonists (10 μM of ADP, 2 μg/mL of collagen, 0.5 mM of arachidonic acid, or 1 U/mL of thrombin), in the presence or absence of peptides, in a final volume of 500 μL with different incubation times (1, 5, and 30 min). The extent of aggregation was estimated quantitatively by measuring the maximum curve height above baseline level. The sample of the suspending medium without any platelets (PPP) was present to serve as a 100% aggregation standard. Concentrations of peptides ranged from 0.01 to 0.2 mg/mL. PRP sample with PBS was used as control to calculate relative magnitude. When thrombin was used, to inhibit fibrin polymerization, 5 μL of 2.0 mmol/L (final concentration) of the peptide glycyl-L-prolyl-L-arginyl-L-prolin (GPRP) was added.

Commercially Available Platelet Concentrate (PRP) from Tianjin Blood Bank. The platelet concentrate was used within its validity period (24 h). The concentration of platelets in platelet concentrate was 10⁸/mL. This PRP was used in the experiments that follow.

Preparation of Platelet-Poor Plasma (PPP) from Commercial Available PRP. The PRP was centrifuged at 1570g for 10 min at 22 °C to acquire PPP.

Determination of Peptide Concentration in Centrifuged Pellet of Platelets by LC-MS. Solutions containing different concentrations of peptides were prepared in PBS with equal molar of sodium carbonate. To 450 μL PRP, 50 μL of peptide solution was added and then incubated at 37 °C for 5 min (final peptide concentrations were 0.035, 0.1, and 0.2 mg/mL). After being centrifuged at 1570g for 10 min, the precipitate was washed 3 times by PBS and then dissolved into 200 μL of DMSO by sonication. The amount of peptides in the platelet precipitate was characterized by LC-MS.

Laser Scanning Confocal Microscopy. The solutions containing 100 mg/mL of Nap-FFG and other peptides were prepared in DMSO and diluted to 2 mg/mL by PBS with equal molar of sodium carbonate. Thioflavin T was added into different peptide solution with 100 μM of the final concentration. The platelets without peptides and peptide solutions without platelets were also stained with equal Thioflavin T as negative controls. 450 μL PRP with or without 50 μL peptide solutions was then incubated at 37 °C for 5 min. After centrifuged at 1570g for 10 min, the solution was washed 3 times by PBS, and resulting platelets were collected into 500 μL PBS. The distribution of different peptides with platelets was observed under laser scanning confocal microscopy (CLSM, Leica TCS SP5).

Cryo-TEM. Cryo-TEM samples (PRP with 0.2 mg/mL Nap-FFG and NapFFA) were prepared at 22 °C and stored at 4 °C. A micropipet was used to load 5 μL sample solution onto a lacey support TEM grid, which was held by tweezers. The excess solution was blotted with a piece of filter paper, resulting in the formation of thin films suspended the mesh holes. After waiting for about 10 s to

relax any stresses induced during the blotting, the samples were quickly plunged into a reservoir of liquid ethane at its melting temperature (−183 °C). The vitrified samples were then stored in liquid nitrogen until they were transferred to a cryogenic sample holder (Gatan 626) and examined with a JEM 2200FS TEM (200 keV) at about −174 °C. The phase contrast was enhanced by under focus. The images were recorded on a Gatan multiscan CCD and processed with Digital Micrographs. TEM was performed on a MODEL H-800 electron microscope operating at an acceleration voltage of 100 kV.

ITC. ITC measurements were performed using a VP-ITC microcalorimeter (MicroCal) in PBS (pH 7.4) at 20 °C. Nap-FFG and four coagulants were dissolved in PBS and adjusted to pH 7.4, then used directly in experiments. To measure the binding constants of thrombin, ADP, AA, and collagen with Nap-FFG, 20 injections of peptide (0.5 mM) into the calorimeter cell, which was completely filled with coagulants solution (1468.5 μL; 0.05 mM), were collected at 180 s intervals while being stirred at 307 rpm. The titration data and binding plot were analyzed using MicroCal Origin software.

ζ Potential. The ζ potential of peptide solutions in PBS or in PRP at 0.2 mg/mL concentration was measured using a BI-90 plus Zetasizer. The measurements were performed automatically using an aqueous dip cell. To prepare the samples of peptide in PRP, the DMSO solution containing 100 mg/mL of peptide was first diluted to 2 mg/mL by PBS with equal molar of sodium carbonate. The solution was then diluted with PRP to make the final peptide concentration to be 0.2 mg/mL.

Determination of Peptide Concentration in Centrifuged Pellet of 3T3 Cells by LC-MS. Solutions containing different concentrations of peptides were prepared in PBS with equal molar of sodium carbonate. To 450 μL Dulbecco's modified Eagle's medium (DMEM) with 10% of FBS containing 3T3 cell (10⁶ cells/mL), 50 μL of peptide solution was added and then incubated at 37 °C for 5 min (final peptide concentrations were 0.035, 0.1, and 0.2 mg/mL). After being centrifuged at 1570g for 10 min, the precipitate was washed 3 times by PBS and then dissolved into 200 μL of DMSO by sonication. The amount of peptides in the 3T3 cells precipitate was characterized by LC-MS.

■ ASSOCIATED CONTENT

📄 Supporting Information

¹H NMR and HR-MS spectra, ¹H NMR peaks assignment, ITC, ζ potentials, concentration of peptide in centrifuged 3T3 cells, CMC of peptides, and inhibition curves. This material is available free of charge via the Internet at <http://pubs.acs.org>.

■ AUTHOR INFORMATION

Corresponding Author

zbli@iccas.ac.cn; kongdeling@nankai.edu.cn; yangzm@nankai.edu.cn

Author Contributions

‡These authors contributed equally.

Notes

The authors declare no competing financial interest.

■ ACKNOWLEDGMENTS

We acknowledge the financial supports from NSFC (50830104 and 51222303). We thank Mr. Xin Zhou from Medical College of Armed Police Forces in Tianjin for his kind help with platelet aggregation examinations. We also thank Prof. Zhenghu Xu at Shandong University for the kind help to assign the NMR peaks of the compounds.

■ REFERENCES

(1) Bowerman, C. J.; Nilsson, B. L. *J. Am. Chem. Soc.* **2010**, *132*, 9526–9527.

- (2) Swaneekamp, R. J.; Dimaio, J. T. M.; Bowerman, C. J.; Nilsson, B. *L. J. Am. Chem. Soc.* **2012**, *134*, 5556–5559.
- (3) Adams, D. J. *Macromol. Biosci.* **2011**, *11*, 160–173.
- (4) Toledano, S.; Williams, R. J.; Jayawarna, V.; Ulijn, R. V. *J. Am. Chem. Soc.* **2006**, *128*, 1070–1071.
- (5) Chen, J.; McNeil, A. J. *J. Am. Chem. Soc.* **2008**, *130*, 16496–16497.
- (6) Bremmer, S. C.; Chen, J.; McNeil, A. J.; Soellner, M. B. *Chem. Commun.* **2012**, *48*, 5482–5484.
- (7) King, K. N.; McNeil, A. J. *Chem. Commun.* **2010**, *46*, 3511–3513.
- (8) Xu, X. D.; Lin, B. B.; Feng, J.; Wang, Y.; Cheng, S. X.; Zhang, X. Z.; Zhuo, R. X. *Macromol. Rapid Commun.* **2012**, *33*, 426–431.
- (9) Soukasene, S.; Toft, D. J.; Moyer, T. J.; Lu, H.; Lee, H.-K.; Standley, S. M.; Cryns, V. L.; Stupp, S. I. *ACS Nano* **2011**, *5*, 9113–9121.
- (10) Altunbas, A.; Lee, S. J.; Rajasekaran, S. A.; Schneider, J. P.; Pochan, D. J. *Biomaterials* **2011**, *32*, 5906–5914.
- (11) Branco, M. C.; Pochan, D. J.; Wagner, N. J.; Schneider, J. P. *Biomaterials* **2010**, *31*, 9527–9534.
- (12) Vemula, P. K.; Cruikshank, G. A.; Karp, J. M.; John, G. *Biomaterials* **2009**, *30*, 383–393.
- (13) Webber, M. J.; Matson, J. B.; Tamboli, V. K.; Stupp, S. I. *Biomaterials* **2012**, *33*, 6823–6832.
- (14) Zhao, F.; Ma, M. L.; Xu, B. *Chem. Soc. Rev.* **2009**, *38*, 883–891.
- (15) Gao, Y.; Kuang, Y.; Guo, Z. F.; Guo, Z. H.; Krauss, I. J.; Xu, B. *J. Am. Chem. Soc.* **2009**, *131*, 13576–13577.
- (16) Jung, J. P.; Moyano, J. V.; Collier, J. H. *Integr. Biol.* **2011**, *3*, 185–196.
- (17) Jayawarna, V.; Ali, M.; Jowitt, T. A.; Miller, A. E.; Saiani, A.; Gough, J. E.; Ulijn, R. V. *Adv. Mater.* **2006**, *18*, 611–617.
- (18) Zhang, S. G. *Nat. Biotechnol.* **2003**, *21*, 1171–1178.
- (19) Haines-Butterick, L.; Rajagopal, K.; Branco, M.; Salick, D.; Rughani, R.; Pilarz, M.; Lamm, M. S.; Pochan, D. J.; Schneider, J. P. *Proc. Natl. Acad. Sci. U.S.A.* **2007**, *104*, 7791–7796.
- (20) Silva, G. A.; Czeisler, C.; Niece, K. L.; Beniash, E.; Harrington, D. A.; Kessler, J. A.; Stupp, S. I. *Science* **2004**, *303*, 1352–1355.
- (21) Standley, S. M.; Toft, D. J.; Cheng, H.; Soukasene, S.; Chen, J.; Raja, S. M.; Band, V.; Band, H.; Cryns, V. L.; Stupp, S. I. *Cancer Res.* **2010**, *70*, 3020–3026.
- (22) Sinthuvanich, C.; Veiga, A. S.; Gupta, K.; Gaspar, D.; Blumenthal, R.; Schneider, J. P. *J. Am. Chem. Soc.* **2012**, *134*, 6210–6217.
- (23) Rudra, J. S.; Sun, T.; Bird, K. C.; Daniels, M. D.; Gasiorowski, J. Z.; Chong, A. S.; Collier, J. H. *ACS Nano* **2012**, *6*, 1557–1564.
- (24) Rudra, J. S.; Tian, Y. F.; Jung, J. P.; Collier, J. H. *Proc. Natl. Acad. Sci. U.S.A.* **2010**, *107*, 622–627.
- (25) Gao, Y.; Long, M. J.; Shi, J.; Hedstrom, L.; Xu, B. *Chem. Commun.* **2012**, *48*, 8404–8406.
- (26) Zheng, W. T.; Wang, Z. H.; Song, L. J.; Zhao, Q.; Zhang, J.; Li, D. X.; Wang, S. F.; Han, J. H.; Zheng, X. L.; Yang, Z. M.; Kong, D. L. *Biomaterials* **2012**, *33*, 2880–2891.
- (27) Wang, Z. H.; Zheng, W. T.; Wang, H. M.; Wang, S. F.; Zhao, Q.; Zhang, J.; Yang, Z. M.; Kong, D. L. *Chem. Commun.* **2011**, *47*, 8901–8903.
- (28) Barre, D. E. *Thromb. Res.* **2007**, *119*, 601–607.
- (29) Sanchez-Cortes, J.; Mrksich, M. *Chem. Biol.* **2009**, *16*, 990–1000.
- (30) Amdursky, N.; Molotskii, M.; Aronov, D.; Adler-Abramovich, L.; Gazit, E.; Rosenman, G. *Nano Lett.* **2009**, *9*, 3111–3115.
- (31) Reches, M.; Gazit, E. *Science* **2003**, *300*, 625–627.
- (32) Freedman, J. E. *Circulation* **2005**, *112*, 2725–2734.
- (33) Maree, A. O.; Fitzgerald, D. J. *Circulation* **2007**, *115*, 2196–2207.
- (34) Raeburn, J.; Pont, G.; Chen, L.; Cesbron, Y.; Levy, R.; Adams, D. J. *Soft Matter* **2012**, *8*, 1168–1174.
- (35) Bieser, A. M.; Tiller, J. C. *Chem. Commun.* **2005**, *31*, 3942–3944.